# Bulletin of the American Meteorological Society


## High-resolution smoke forecasting for the 2018 Camp Fire in California

--Manuscript Draft--

| | |
|---|---|
| **Manuscript Number:** | BAMS-D-20-0329 |
| **Full Title:** | High-resolution smoke forecasting for the 2018 Camp Fire in California |
| **Article Type:** | Article |
| **Order of Authors:** | Fotini Katopodes Chow, Ph.D. |
| | Katelyn A. Yu |
| | Alexander Young |
| | Eric James |
| | Georg Grell |
| | Ivan Csiszar |
| | Marina Tsidulko |
| | Saulo Freitas |
| | Gabriel Pereira |
| | Louis Giglio |
| | Ravan Ahmadov |
| **Manuscript Classifications:** | 4.192: Dispersion; 8.148: Numerical weather prediction/forecasting; 8.196: Tracers; 10.012: Air quality; 10.104: Forest fires; 12.144: Wildfires |
| **Abstract:** | Smoke from the 2018 Camp Fire in Northern California blanketed a large part of the region for two weeks, creating poor air quality in the “unhealthy” range for millions of people. The NOAA Global System Laboratory's HRRR-Smoke model was operating experimentally in real time during the Camp Fire. Here, output from the HRRR-Smoke model is compared to surface observations of PM2.5 from the AirNow and Purple Air sensors, in addition to meteorological and satellite observation data. The HRRR-Smoke model grid at 3-km resolution simulated successfully the evolution of the plume at low levels (down-valley winds) and upper levels (east winds) during the initial phase of the fire (8-9 November 2018). During the second week (15-16 November), HRRR-Smoke was able to capture the intensification of PM2.5 pollution due to a high pressure system and subsidence that trapped smoke close to the surface; however, HRRR-Smoke underpredicted PM2.5 levels in the latter half of the event due to likely underestimates of the fire radiative power derived from satellite observations. The intensity of the Camp Fire smoke event and the resulting pollution during the stagnation episodes make it an excellent test case for HRRR-Smoke in predicting PM2.5 levels, which were so high from this single fire event that the usual anthropogenic pollution sources became insignificant. The analysis of this pollution episode can also help to improve air quality forecasts in the future. The HRRR-Smoke model was implemented operationally at NOAA/NCEP in December 2020, now providing essential support for smoke forecasting as the impact of US wildfires continues to increase in scope and magnitude. |

# High-resolution smoke forecasting for the 2018 Camp Fire in California

Fotini Katopodes Chow, Katelyn A. Yu, Alexander Young*

*Civil and Environmental Engineering, University of California, Berkeley, Berkeley, California*

Eric James

*CIRES, University of Colorado, Boulder, Colorado*

*NOAA Global Systems Laboratory, Boulder, Colorado*

Georg Grell

*NOAA Global Systems Laboratory, Boulder, Colorado*

Ivan Csiszar

*Center for Satellite Applications and Research, NOAA National Environmental Satellite, Data, and Information Service, College Park, Maryland*

Marina Tsidulko

*I.M. Systems Group, Rockville, Maryland*

Saulo Freitas

*Universities Space Research Association, Columbia, Maryland*

*Global Modeling and Assimilation Office, NASA/GSFC, Greenbelt, Maryland*

Gabriel Pereira

*Department of Geosciences, Federal University of Sao Joao del-Rei, Sao Joao del-Rei, Brazil*

Louis Giglio

*Geographical Sciences, University of Maryland, College Park, Maryland*

Ravan Ahmadov[†]

*CIRES, University of Colorado, Boulder,Colorado*

*NOAA Global Systems Laboratory, Boulder, Colorado*

[*]Current affiliation: Cornell University, Ithaca, New York

[†]*Corresponding author*: Ravan Ahmadov, ravan.ahmadov@noaa.gov

ABSTRACT

Smoke from the 2018 Camp Fire in Northern California blanketed a large part of the region for two weeks, creating poor air quality in the "unhealthy" range for millions of people. The NOAA Global System Laboratory's HRRR-Smoke model was operating experimentally in real time during the Camp Fire. Here, output from the HRRR-Smoke model is compared to surface observations of PM2.5 from the AirNow and Purple Air sensors, in addition to meteorological and satellite observation data. The HRRR-Smoke model grid at 3-km resolution simulated successfully the evolution of the plume at low levels (down-valley winds) and upper levels (east winds) during the initial phase of the fire (8-9 November 2018). During the second week (15-16 November), HRRR-Smoke was able to capture the intensification of PM2.5 pollution due to a high pressure system and subsidence that trapped smoke close to the surface; however, HRRR-Smoke underpredicted PM2.5 levels in the latter half of the event due to likely underestimates of the fire radiative power derived from satellite observations. The intensity of the Camp Fire smoke event and the resulting pollution during the stagnation episodes make it an excellent test case for HRRR-Smoke in predicting PM2.5 levels, which were so high from this single fire event that the usual anthropogenic pollution sources became insignificant. The analysis of this pollution episode can also help to improve air quality forecasts in the future. The HRRR-Smoke model was implemented operationally at NOAA/NCEP in December 2020, now providing essential support for smoke forecasting as the impact of US wildfires continues to increase in scope and magnitude.

*Capsule summary.* NOAA's HRRR-Smoke model captured the intense smoke pollution and its spatial distribution from the 2018 Camp Fire in Northern California when smoke blanketed the region for two weeks.

## 1. Introduction

Major wildfire events have increasingly intersected with urban communities in recent years. Apart from wildfires crossing the wildland-urban interface, wildfire smoke can affect communities hundreds of miles away. The Camp Fire, which started on 8 November 2018 near Paradise, CA, is a prime example of an event which had inordinate effects on regional air quality and visibility. The Camp Fire destroyed almost 19,000 structures, killed 88 people (California's deadliest fire to date), and displaced over 50,000 people from their homes (Ban et al. 2020; Palinkas 2020). In addition, millions of people in Northern California were exposed to poor air quality for many days, with potential health impacts including increased mortality and other health complications (Palinkas 2020; Balmes 2020; Holm et al. 2021; Reid et al. 2016; Wettstein et al. 2018; Liu et al. 2017). Similarly, multi-week air quality impacts were seen during the 2020 fire season due to numerous large wildfires throughout the Western United States (CBS San Francisco 2020; The Mercury News 2020).

Air quality forecast guidance is typically produced by the Environmental Protection Agency and local offices, such as the California Air Resources Board (CARB) or the Bay Area Air Quality Management District (BAAQMD), and disseminated through the `airnow.gov` website. During the Camp Fire, this website was inundated with traffic, rendered unavailable (Knobel 2018), and was only able to report coarse spatial patterns in the estimated air quality index (AQI) based on sparsely distributed air quality sensors. The smoke from the Camp Fire reached the San Francisco Bay Area, with a population of about 8 million people, within hours of fire ignition. The smoke persisted for about 2 weeks, in many places intensifying during the middle of this period due to a high pressure system with subsidence and shallow mixing layer heights. On 10 November 2018 (the third day of the Camp Fire), PM2.5 levels reached "unhealthy" levels (151-200 AQI) for the whole Bay Area. On 16-18 November, Bay Area air quality worsened further and was reported to be among the worst in the world, with the air quality index (AQI) reaching higher than 250 in San Francisco, prompting widespread school closures (Coren 2018).

High-resolution smoke forecasts are needed to provide reliable spatial and temporal information during extreme wildfire events. NOAA has been running the High-Resolution Rapid Refresh (HRRR) model at 3 km grid spacing to provide hourly convection-permitting weather forecasts over the entire continental US (Benjamin et al. 2016). Since its operational implementation in 2014, the HRRR has become an essential tool for weather forecasters. It is widely used for predicting hazardous weather in applications ranging from severe thunderstorms and heavy rainfall to low cloud ceilings and reduced visibility (see e.g. Benjamin et al. 2021). In 2016, a single smoke tracer (primary PM2.5, based on Grell et al. (2011)), a plume rise parameterization (Freitas et al. 2007, 2010), and satellite fire radiative power processing (Ahmadov et al. 2017) were implemented in an experimental version of the HRRR model, referred to as the HRRR-Smoke model. During the Camp Fire event, HRRR-Smoke was operated in real-time demonstration mode by the NOAA Global Systems Laboratory (GSL) with graphical forecast output available online (`https://rapidrefresh.noaa.gov/hrrr/HRRRsmoke/`). The HRRR-Smoke model became fully operational at NOAA/NCEP in December 2020.

Here we examine the ability of the HRRR-Smoke model to capture the smoke plumes generated by the 2018 Camp Fire to produce PM2.5 forecasts for affected communities. The HRRR-Smoke model has recently been evaluated in a model intercomparison study for the 2019 Williams Flats fire (Ye et al. 2021). For the present study, the model has been re-run for the Camp Fire case using a more recent version of the code (HRRRv4, implemented operationally in December 2020) to better evaluate its forecasting abilities for such an exceptional air quality event. Model outputs are compared to data from the AirNow and Purple Air community air quality sensors, meteorological station data, and to satellite observations.

This paper presents the first in-depth analysis of the ability of the HRRR-Smoke coupled weather-smoke model to provide smoke forecasting at 3 km resolution, which is a major milestone for a model with a domain of this size (covering the continental US). The coupled modeling framework and hourly refresh cycle make HRRR-Smoke a powerful tool for forecasting such extreme smoke pollution events. The Camp Fire is an excellent case study due to the relatively clean background air (no other major wildfires in the western US) and the very high concentrations of smoke, which persisted over the region for an extended time period. The Camp Fire occurred during November, also making this a unique smoke event compared to summertime, when multiple wildfires typically affect air quality across urban areas in the Western US. Combined with a dense network of sensors (AirNow and Purple Air), this study of the 2018 Camp Fire also provides an opportunity to envision a more accurate forecast system that could ultimately be combined with real-time data to give communities better predictions during smoke events.

The National Weather Service report from the Camp Fire recommended "a consistent source of smoke transport model guidance (e.g. HRRR-Smoke)" to provide reliable forecasts and messaging (National Weather Service Western Region Headquarters 2020). This model guidance will be especially useful as the frequency of wildfire events near urban areas increases due to climate change (such as the fire incidents in the Western US in 2019, 2020, and 2021) and also for managing prescribed burns designed to prevent catastrophic wildfires (Miller et al. 2020). Improved forecasts, combined with dense networks of community-installed air quality sensors, will enable government agencies to give better guidance about smoke exposure to help protect disadvantaged communities and at-risk individuals and to help better plan hospital emergency room demand. Predictions with increased spatial resolution will also provide more accurate guidance about limiting outdoor activities. In addition, weather prediction models can be improved by including smoke impacts on solar radiation reaching the surface; HRRR-Smoke has this capability, but most other weather prediction models do not, which can lead to large forecast errors during intense smoke events (NESDIS 2021).

This paper begins with a description of the smoke plume evolution during the first few days of the Camp Fire event with comparisons to air quality monitors (Section 2), followed by comparison with meteorological observations (Section 3). The paper concludes with a comparison to satellite observations, including a discussion of model errors and future areas of research related to satellite fire detection algorithms (Section 4).

## 2. Spatial evolution of winds and smoke

Figure 1 shows the dramatic spread of wildfire smoke from the Camp Fire across Northern California, with snapshots of HRRR-Smoke PM2.5 concentrations overlaid with wind vectors. Images are shown at three hourly intervals for 3-12 hours after the time the fire was initialized in the model, at the surface and aloft. Details of the HRRR-Smoke model configuration are provided in the Appendix. Near the ground, the east winds over the Sierras moved smoke into the Central Valley where downvalley winds pushed the smoke southward toward the Bay Area. Aloft, the strong NNE winds drove the smoke across the Central Valley to the coastal mountain range. Continued NNW winds along the Central Valley created a V-shape in the near-surface smoke plume, as seen in Fig. 1.

The smoke prediction from HRRR-Smoke is dependent on the ingested satellite fire detections. The Camp Fire began around 1430 UTC 8 November 2018 (6:30am local time) National Weather

Service Western Region Headquarters (2020). The MODIS instrument onboard the Terra satellite detected the fire about 4 hours later at 1810 UTC (10:10am local time). The HRRR-Smoke model therefore lags the observations by several hours on the day of the fire ignition, but is nevertheless able to capture the relative timing of the smoke arrival at different locations. Ingesting the geostationary satellite FRP data into the model could help to mitigate this detection delay issue in the future (O'Neill and Raffuse 2021), as described further in Section 4. As wildfires can start any time or evolve rapidly, it is important to ingest the satellite detections into the smoke forecast models with the shortest delay possible. Because new HRRR forecasts start every hour by assimilating the latest meteorological observations, this framework also allows ingesting the "latest" FRP detections into the model.

Fig. 2 shows a snapshot of surface winds and smoke concentrations from HRRR-Smoke compared to surface PM2.5 measurements from both AirNow and Purple Air sensors. There is good qualitative agreement between HRRR-Smoke and the collection of PM2.5 sensors. The Purple Air community-based sensors provide more spatially detailed PM2.5 data with significantly less expensive sensors. These sensors have been validated in a few studies, *e.g.* Gupta et al. (2018) who found that while the sensors are not as accurate as the quality-controlled AirNow sensors, they do capture trends and spatial variability. The Purple Air sensors used for comparison to HRRR-Smoke were filtered by removing indoor sensors and sensors with missing data as described in the Appendix.

A more detailed comparison with surface observations for selected sensors (locations shown in Figure 3) illustrates the ability of HRRR-Smoke to capture the smoke plume spread. Fig. 4 shows several time series of PM2.5 concentrations at various distances along the main direction of the smoke plume: Sacramento (south of Paradise), East Bay (further west), and South Bay (further south). The PurpleAir sensors recorded 2-3 hr shifts in the arrival of the smoke plume at each subsequent location, and these time shifts are well captured by the HRRR-Smoke model, albeit delayed by about 4 hours due to late initiation of the fire in the model. Comparisons between selected individual high-quality AQS sensors and HRRR-Smoke output in Fig. 5 show similar agreement between the model and the AQS observations. The shifted arrival times of the smoke plume are seen again here. The delay in the modeled smoke arrival time is also visible above in the contour plots of surface PM2.5 concentration from HRRR-Smoke with Purple Air and AirNow sensors in Fig. 2, and in Supplemental Material Fig. S1 for 3-24 hours after the fire initialization in the model, where the sensors generally show higher values (brighter colors) in the earlier hours of the simulation, compared to HRRR-Smoke.

Further intensification of the smoke event during the second week illustrates the complex interaction of meteorology and emissions and points to the need for improved models and observations which can capture these details. Figure 6 shows a time series of PM2.5 concentration from EPA monitoring sites in Pleasanton and Oakland over the entire two-week duration of the smoke event in the Bay Area, 8-21 November 2018. This plot is shown with a linear concentration axis to highlight two things: first, that after some initial improvement on days 3-6, there is a distinct worsening of air quality during days 7-9 of the event (14-16 November 2018), and second, that the HRRR-Smoke model in general underpredicts concentrations, likely due to significant underestimations in the FRP data (see Section 4). It appears that the reduction in smoke during the intermediate period from 11-14 November 2018 occurred because winds shifted to weak southerly, which pushed the smoke plume to the north. When winds shifted again to the NNW, the plume brought new smoke toward the Bay Area, which when combined with subsidence and a very stable capping inversion, led to very high near-surface concentrations of PM2.5. This worsening of air quality prompted widespread school closures in the Bay Area with the highest ever recorded AQI values of 256 observed in Oakland and 271 in San Francisco on 16 November 2018. (SFGATE

2018). HRRR-Smoke captures the sharp increase in PM2.5 values at the start of this intensification period, though again with some delay, but greatly underpredicts smoke values for the duration of the Camp Fire smoke event.

## 3. Comparison to meteorological observations

To further explain the observed behavior of the smoke plume in observations and in the model, we examine the meteorological conditions driving the smoke event, including surface observations and vertical profiles. The Camp Fire event was characterized by an east-west surface pressure gradient causing very strong downslope winds combined with very dry conditions (very low relative humidity, 10% during the day and in the teens at night). Wind speeds were 12-14 m/s, and a 23 m/s (52 mph) gust was recorded at the Jarbo Gap site near Paradise, CA early that morning (National Weather Service Western Region Headquarters 2020). A detailed analysis of synoptic flow conditions is found in Brewer and Clements (2020).

Time series and vertical sounding comparisons of surface temperatures, wind speed and direction, confirm that HRRR-Smoke matched observations quite well. Fig. 7 shows the vertical sounding upwind at Reno, NV indicating stable conditions at night (1200 UTC = 4:00am local time) with a capping inversion near mountain crest height, winds from the East, and a very dry boundary layer, leading to the downslope windstorm which fueled the Camp Fire on the lee side of the ridge (Brewer and Clements 2020). During the day (0000 UTC = 4:00pm local time) a mixed layer develops with stable conditions aloft and low moisture persisting. Profiles of smoke concentration (mass density) are negligibly small in Reno, located upwind of the fire (only wildfire sources of PM2.5 are included in HRRR-Smoke). In the Oakland soundings in Fig. 7, we see a set of layered stable regions near the ground at night and a mixed layer during the day, with winds largely from the Northeast. The boundary layer is quite dry, with the model overpredicting specific humidity.

The smoke concentration increases to over 50 $\mu$g/m$^3$ at the surface on 1200 UTC 9 November (not shown). By 15-16 November, with very weak winds and very stable conditions near the ground even during the daytime, smoke concentrations in Oakland are 50 $\mu$g/m$^3$ at the surface and have increased to more than 100 $\mu$g/m$^3$ at about 1 km ASL (Figure 8). These comparisons, in addition to the corresponding 0000 UTC comparisons shown in the supplemental Figures S2-S3, demonstrate the relatively good agreement between HRRR and the observed profiles.

Figure 9 shows time series for the first few days of the Camp Fire of wind speed, direction, and temperature at Reno and at two stations near Paradise, namely, Jarbo Gap on the slope, and Openshaw in the valley, shown in Fig. 3. Again the model shows good agreement with observations, capturing the NE wind direction (~45°) during 06-12 UTC and later the increasing wind speeds at Reno upwind of the Sierras. Time series at Jarbo Gap, near the location of the fire, show the dramatic increase in winds on the downslope side of the Sierras, of 12-14 m/s from 0600 to 1200 UTC 8 November coming from the NE. At the Openshaw station, located south of Chico in the Central Valley, winds were down valley from the NNW with periodic interruptions of NNE downslope flows from the Sierra Nevada range. Further analysis and quantification of model errors compared to observations are included in the Appendix.

## 4. Satellite observations: model comparisons and detection challenges

The meteorological variables are captured very well by HRRR-Smoke at 3 km resolution over the complex terrain of the Western US, as seen by the foregoing discussion and further analysis included in the Appendix. The evolution of the smoke concentration is also well represented by HRRR-Smoke, considering the complexity of the domain and the uncertainties regarding the fire detection and forecasting the fire emissions and spread. Figure 10 shows comparisons of the vertically integrated smoke and VIIRS satellite images captured in the afternoon on selected dates (a video is included in the Supplemental Material). Qualitative agreement is best at the beginning of the time period, and the images show remarkable similarities in the smoke plume structures, including the initial high-altitude spread of the plume on 8 November, the V-shaped structure on 9 November, the thick smoke concentrated near Paradise on 12 November, and the stagnant smoke that settles over the Central Valley and the Bay Area around 15 November. By 12 and 15 November, as seen earlier in Figure 5, the agreement of the HRRR-Smoke PM2.5 concentrations with observations has decreased, with the model showing a significantly lower PM2.5 concentration spread over California.

HRRR-Smoke represents wildfires by surface fluxes prescribed by satellite detection of fire radiative power (FRP) (Ahmadov et al. 2017). A plume rise model also plays a vital role in injecting smoke directly into the free troposphere (Freitas et al. 2007, 2010). Figure 11 shows time series of the FRP data ingested from polar orbiting satellites during the Camp Fire event, showing the dramatic decrease in FRP after 8 November. The FRP is retrieved for pixels flagged as *fire* in the VIIRS I-band and 1-km MODIS fire products (Li et al. 2018). The daily sequence of daytime Suomi NPP images shows a good delineation of the fire front of the Camp Fire event between 8-12 November (see Supplemental Material, Figure S4). On 13 November, however, no daytime detections were reported by the algorithm due to persistent (though not totally opaque) cloud cover. NOAA-20 and Terra/Aqua FRP data (not shown) follow similar patterns. (For MODIS imagery, visit NASA EOSDIS Worldview at `https://worldview.earthdata.nasa.gov/`). Because the fire intensities are usually high during daytime, such omissions of the satellite FRP data entirely during the daytime leads to very low biomass burning flux estimates ingested into the model. The HRRR-Smoke model cycles smoke between subsequent forecasts, therefore the following forecast cycles are also impacted by the daytime FRP omission on November 13. From 14-20 November, daytime detections were reported again by the algorithm, but with the omission of some areas of active burning. Nighttime detections (not shown) provided more complete spatial coverage of the areas of active burning throughout the entire time period of 8-20 November analyzed. The loss of detection of active burning during the daytime in this instance is likely the result of an increase in near-infrared reflectance from heavy smoke, which can trigger various internal non-fire tests within the detection algorithm which exclude the pixel from further consideration as possibly containing a fire. In contrast, very windy conditions tend to push thick smoke away from the path of radiance between the fire and the satellite sensor and hence allow for a more unobstructed observation of the fire; this increases the likelihood of detection and FRP retrieval. Such windy conditions were observed in particular on 8-9 and 12 November, with relative drops in FRP recorded in between (see Figure 11).

## 5. Conclusions and future work

With wildfires now creating large-scale smoke events which regularly affect large populations in the Western US, the need for a robust wildfire smoke prediction model like HRRR-Smoke is clear. The 2018 Camp Fire event allowed detailed comparison of PM2.5 from the wildfire smoke with AirNow and Purple Air observations to validate HRRR-Smoke because of the very low background PM2.5 levels during that time period. HRRR-Smoke captured the meteorology very well and hence captured the qualitative spatial structure of the smoke (Fig. 10) over Northern California, particularly during the first few days of the Camp Fire event. The HRRR-Smoke model also includes smoke feedback on meteorology, which helped to capture the stagnation event during the second week of the event. Comparisons to new dense surface station networks from PurpleAir and AirNow allowed spatial patterns in smoke evolution to be verified.

One of the limitations of the HRRR-Smoke model is its reliance on relatively infrequent and possibly degraded observations of fire radiative power derived from satellite observations. The satellite FRP was underpredicted during the second half of the smoke event. The VIIRS data at 375 m resolution is the highest resolution instrument for satellite fire detection, thus with respect to sensitivity and spatial fidelity VIIRS imagery will often be the source of choice for FRP data. However, at present only data from polar orbiting satellites are employed in the model, reducing sampling frequency to a few daytime and a few nighttime observations. Inclusion of data from the geostationary GOES-R platforms will significantly improve temporal coverage (O'Neill and Raffuse 2021). Another approach to account for FRP errors would be to use source inversion modeling based on the dense surface station networks, to automatically adjust the smoke emissions from the fires (see e.g. Li et al. 2020). Additionally, data assimilation can be used to compensate for errors in the source terms. For instance, assimilating the surface PM2.5 measurements in conjunction with the satellite aerosol optical depth data into the smoke forecasting models can improve the accuracy of the smoke forecasts in the future (Saide et al. 2014). Emerging comparisons with ceilometer data will also allow better evaluation of the vertical structure of wildfire smoke plumes (Huff et al. 2021).

HRRR-Smoke is becoming an essential tool for providing real-time operational support for weather and air quality forecasters. Because the model includes radiation feedback from the smoke which affects surface temperatures, it is able to capture smoke-induced events like the "orange skies" seen in California lightning complex fires of August 2020 (NESDIS 2021). HRRR-Smoke currently restarts hourly, which allows it to ingest new satellite detection data at a very high frequency compared to other air quality models. Further validation and improvement of the model are needed to enable more accurate prediction of wildfire or prescribed burn smoke events for community health and safety. Ultimately, modeling and sensor networks can be combined to provide robust nowcasts and forecasts for poor air quality events due to wildfire smoke.

## 6. Acknowledgements

Ravan Ahmadov and Eric James thank the JPSS PGRR program for funding the HRRR-Smoke model development. We thank Johana Romero-Alvarez for processing the satellite FRP time series for the Camp fire. The authors thank the HRRR team for contributing to the model development.

*Data availability statement.* The model data that support the findings of this study are available from the corresponding author upon reasonable request and/or from the HRRR-Smoke website (`https://rapidrefresh.noaa.gov/hrrr/HRRRsmoke/`). The meteorological and air quality data that support the findings of this study are publicly available from Purple Air (`https://api.purpleair.com`), AirNow (`https://gispub.epa.gov/airnow/index.html?tab=3`), NOAA RAWS (`https://wrcc.dri.edu/wraws/ccaF.html`), and satellite images from NOAA NESDIS JSTAR Mapper (`https://www.star.nesdis.noaa.gov/jpss/mapper/`) websites.

## APPENDIX

### Model

The HRRR is an hourly data assimilation and weather forecast forecast system. Some details of the HRRR configuration differ between what was running in real-time in 2016 vs. what was run retrospectively (in forecast mode) for this study. The retrospective simulations used for this study carried out hybrid ensemble 3DVar data assimilation for meteorology (Hu et al. 2017) based on the community Gridpoint Statistical Interpolation (GSI, Kleist et al. 2009). Background error covariances are a blend of ensemble covariances from the 80-member Global Data Assimilation System (GDAS) ensemble and static covariances (Wang 2010). Many conventional observations are assimilated hourly in a manner analogous to the 13 km Rapid Refresh (RAP) system (Benjamin et al. 2016). However, in the HRRR, the background for the data assimilation comes from a 1 h “pre-forecast" in which 15-min radar reflectivity observations are assimilated. The“pre-forecast" is initialized from a downscaled RAP 0-h analysis; boundary conditions for both the “pre-forecast" and full forecast come from the RAP. The model component of the HRRR is based on WRF-ARW (Powers et al. 2017), with advanced physics parameterizations (Benjamin et al. 2016). For the retrospective analysis done here, HRRR was rerun at 6-hr forecast intervals to conserve computational resources. Frequent restarts are important to capture the onset of the fire, where MODIS Terra detected it at 1810 UTC 8 November (10:10am local time), and HRRR ingested it. The retrospective forecast was done using VIIRS I-band (375 m resolution) as input as opposed to M-band (750 m resolution) which was used in the real-time modeling.

Figure A1 shows time series of model 10-m wind bias and RMSE compared to all METAR surface stations in the Northwest continental US during the entire duration of the Camp Fire. Absolute bias values are generally below 0.5 m/s, and RMSE generally stays below 3 m/s except during 14-16 November when the peak errors of 3.3 m/s occur during the daytime for the 12-h and 18-h forecasts; the timing of these peak errors corresponds to the passage of upper-level shortwave troughs across British Columbia. The 6-h forecast performs considerably better throughout the entire period, both in terms of bias and RMSE, illustrating the benefit of frequent data assimilation. Similar statistics (not shown) are found in comparisons to upper air observations (radiosondes). These statistics, combined with detailed comparisons at specific locations (as seen in Figures 7-9) confirm that the meteorological representation from HRRR-Smoke was overall in good agreement with surface and upper air observations.

A final additional comparison of model output and observations is offered in Fig. A2, which compares ceilometer observations with vertical profiles of PM2.5 from HRRR-Smoke. We can see elevated layers of smoke that sometimes correspond with ceilometer cloud levels. Raw ceilometer data (which were unavailable for this study) may be able to provide greater granularity in characterizing elevated smoke layers in the future (National Research Council 2009; Huff et al. 2021).

### Sensors

The PurpleAir network consists of low-cost PM2.5 sensors, predominantly marketed for monitoring local air quality near homes or work places. The low cost of the sensors has increased their rate of adoption and created a relatively dense real-time air quality sensor network in and around the populated areas of California. Direct comparisons with groups of PurpleAir sensors in the Bay Area were made in three areas of interest with adequate density of PurpleAir sensors: East Bay, South Bay, and Sacramento. High sensor densities in these three areas increase the robustness of the comparison with the HRRR-Smoke model.

Publicly maintained low-cost air sensors are subject to more errors than the AQS sensors maintained by air quality agencies. Common issues with the low-cost sensors include data gaps, extremely high or low values, and some loss of accuracy in high relative humidity and high coarse particle concentration conditions (Stavroulas et al. 2020). To minimize any such errors, focusing on areas with dense sensor networks ensured that individual sensors could be compared to the aggregate network to remove outliers. Further, any sensors with gaps in data over the time period of interest were removed. Finally, the two separate channels on the PurpleAir sensors were compared to determine if the sensor had any technical issues causing internal discrepancies.

Using these constraints to filter the Purple Air data, the average HRRR-Smoke data could be compared to the average Purple Air data from sensors within each area (Figure 4). While AQS sensors provide more reliable information, the density of the AQS network was not high enough to generate a fair comparison between city AQS sensors and the average HRRR value. As a result, we opted instead to compare individual AirNow sensors with their closest gridded HRRR data point (Figures 5 and 6).

## References

Ahmadov, R., and Coauthors, 2017: Using VIIRS fire radiative power data to simulate biomass burning emissions, plume rise and smoke transport in a real-time air quality modeling system. *2017 IEEE International Geoscience and Remote Sensing Symposium (IGARSS)*, 2806–2808, doi:10.1109/IGARSS.2017.8127581, iSSN: 2153-7003.

Balmes, J. R., 2020: The Changing Nature of Wildfires: Impacts on the Health of the Public. *Clinics in Chest Medicine*, **41 (4)**, 771–776, doi:10.1016/j.ccm.2020.08.006, URL https://www.sciencedirect.com/science/article/pii/S0272523120300812.

Ban, Y., P. Zhang, A. Nascetti, A. R. Bevington, and M. A. Wulder, 2020: Near Real-Time Wildfire Progression Monitoring with Sentinel-1 SAR Time Series and Deep Learning. *Scientific Reports*, **10 (1)**, 1322, doi:10.1038/s41598-019-56967-x, URL https://www.nature.com/articles/s41598-019-56967-x, number: 1 Publisher: Nature Publishing Group.

Benjamin, S. G., and Coauthors, 2016: A North American Hourly Assimilation and Model Forecast Cycle: The Rapid Refresh. *Monthly Weather Review*, **144 (4)**, 1669–1694, doi:10.1175/MWR-D-15-0242.1, URL https://journals.ametsoc.org/view/journals/mwre/144/4/mwr-d-15-0242.1.xml, publisher: American Meteorological Society Section: Monthly Weather Review.

Benjamin, S. G., and Coauthors, 2021: Stratiform Cloud-Hydrometeor Assimilation for HRRR and RAP Model Short-Range Weather Prediction. *Monthly Weather Review*, **-1 (aop)**, doi:10.1175/MWR-D-20-0319.1, URL https://journals.ametsoc.org/view/journals/mwre/aop/MWR-D-20-0319.1/MWR-D-20-0319.1.xml, publisher: American Meteorological Society Section: Monthly Weather Review.

Brewer, M. J., and C. B. Clements, 2020: The 2018 Camp Fire: Meteorological Analysis Using In Situ Observations and Numerical Simulations. *Atmosphere*, **11 (1)**, 47, doi: 10.3390/atmos11010047, place: Basel Publisher: Mdpi WOS:000516826200047.

CBS San Francisco, 2020: Wind Shift Returns Smoky Haze To San Francisco Bay Area Skies. URL https://sanfrancisco.cbslocal.com/2020/10/10/wind-shift-returns-smoky-haze-to-san-francisco-bay-area-skies/.

Coren, M. J., 2018: California's air was among the world's worst this week. Climate change will make it the new normal. URL https://qz.com/1466111/californias-air-was-among-the-worlds-worst-this-week-climate-change-makes-that-the-new-normal/, library Catalog: qz.com.

Freitas, S. R., K. M. Longo, J. Trentmann, and D. Latham, 2010: Technical Note: Sensitivity of 1-D smoke plume rise models to the inclusion of environmental wind drag. *Atmospheric Chemistry and Physics*, **10 (2)**, 585–594, doi:https://doi.org/10.5194/acp-10-585-2010, URL https://acp.copernicus.org/articles/10/585/2010/, publisher: Copernicus GmbH.

Freitas, S. R., and Coauthors, 2007: Including the sub-grid scale plume rise of vegetation fires in low resolution atmospheric transport models. *Atmospheric Chemistry and Physics*, **7 (13)**, 3385–3398, doi:10.5194/acp-7-3385-2007, URL https://acp.copernicus.org/articles/7/3385/2007/, publisher: Copernicus GmbH.

Grell, G., S. R. Freitas, M. Stuefer, and J. Fast, 2011: Inclusion of biomass burning in WRF-Chem: impact of wildfires on weather forecasts. *Atmospheric Chemistry and Physics*, **11 (11)**, 5289–5303, doi:10.5194/acp-11-5289-2011, URL https://acp.copernicus.org/articles/11/5289/2011/, publisher: Copernicus GmbH.

Gupta, P., and Coauthors, 2018: Impact of California Fires on Local and Regional Air Quality: The Role of a Low-Cost Sensor Network and Satellite Observations. *GeoHealth*, **2 (6)**, 172–181, doi:10.1029/2018GH000136, URL https://agupubs.onlinelibrary.wiley.com/doi/abs/10.1029/2018GH000136, _eprint: https://agupubs.onlinelibrary.wiley.com/doi/pdf/10.1029/2018GH000136.

Holm, S. M., M. D. Miller, and J. R. Balmes, 2021: Health effects of wildfire smoke in children and public health tools: a narrative review. *Journal of Exposure Science and Environmental Epidemiology*, **31 (1)**, 1–20, doi:10.1038/s41370-020-00267-4, place: London Publisher: Springernature WOS:000571372200001.

Hu, M., S. G. Benjamin, T. T. Ladwig, D. C. Dowell, S. S. Weygandt, C. R. Alexander, and J. S. Whitaker, 2017: GSI Three-Dimensional Ensemble–Variational Hybrid Data Assimilation Using a Global Ensemble for the Regional Rapid Refresh Model. *Monthly Weather Review*, **145 (10)**, 4205–4225, doi:10.1175/MWR-D-16-0418.1, URL https://journals.ametsoc.org/view/journals/mwre/145/10/mwr-d-16-0418.1.xml, publisher: American Meteorological Society Section: Monthly Weather Review.

Huff, A. K., S. Kondragunta, H. Zhang, I. Laszlo, M. Zhou, V. Caicedo, R. Delgado, and R. Levy, 2021: Tracking Smoke from a Prescribed Fire and Its Impacts on Local Air Quality Using Temporally Resolved GOES-16 ABI Aerosol Optical Depth (AOD). *Journal of Atmospheric and Oceanic Technology*, **38 (5)**, 963–976, doi:10.1175/JTECH-D-20-0162.1, URL https://journals-ametsoc-org.libproxy.berkeley.edu/view/journals/atot/aop/JTECH-D-20-0162.1/JTECH-D-20-0162.1.xml, publisher: American Meteorological Society Section: Journal of Atmospheric and Oceanic Technology.

Kleist, D. T., D. F. Parrish, J. C. Derber, R. Treadon, W.-S. Wu, and S. Lord, 2009: Introduction of the GSI into the NCEP Global Data Assimilation System. *Weather and Forecasting*, **24 (6)**, 1691–1705, doi:10.1175/2009WAF2222201.1, URL https://journals.ametsoc.org/view/journals/wefo/24/6/2009waf2222201_1.xml, publisher: American Meteorological Society Section: Weather and Forecasting.

Knobel, L., 2018: Unhealthy air quality caused by Camp Fire persists in Berkeley. URL https://www.berkeleyside.com/2018/11/12/unhealthy-air-quality-caused-by-camp-fire-persists-in-berkeley.

Li, F., X. Zhang, S. Kondragunta, and I. Csiszar, 2018: Comparison of Fire Radiative Power Estimates From VIIRS and MODIS Observations. *Journal of Geophysical Research: Atmospheres*, **123 (9)**, 4545–4563, doi:https://doi.org/10.1029/2017JD027823, URL https://agupubs.onlinelibrary.wiley.com/doi/abs/10.1029/2017JD027823, _eprint: https://agupubs.onlinelibrary.wiley.com/doi/pdf/10.1029/2017JD027823.

Li, Y., and Coauthors, 2020: Ensemble PM2.5 Forecasting During the 2018 Camp Fire Event Using the HYSPLIT Transport and Dispersion Model. *Journal of Geophysical Research: Atmospheres*, **125 (15)**, e2020JD032 768, doi:10.1029/2020JD032768, URL https://agupubs.onlinelibrary.wiley.com/doi/abs/10.1029/2020JD032768, _eprint: https://agupubs.onlinelibrary.wiley.com/doi/pdf/10.1029/2020JD032768.

Liu, J. C., and Coauthors, 2017: Wildfire-specific Fine Particulate Matter and Risk of Hospital Admissions in Urban and Rural Counties. *Epidemiology (Cambridge, Mass.)*, **28 (1)**, 77–85, doi:10.1097/EDE.0000000000000556, URL https://www.ncbi.nlm.nih.gov/pmc/articles/PMC5130603/.

Miller, R. K., C. B. Field, and K. J. Mach, 2020: Barriers and enablers for prescribed burns for wildfire management in California. *Nature Sustainability*, **3 (2)**, 101–109, doi: 10.1038/s41893-019-0451-7, URL http://www.nature.com/articles/s41893-019-0451-7, number: 2 Publisher: Nature Publishing Group.

National Research Council, 2009: *Observing Weather and Climate from the Ground Up: A Nationwide Network of Networks*. The National Academies Press, Washington, DC, doi:10.17226/12540, URL https://www.nap.edu/catalog/12540/observing-weather-and-climate-from-the-ground-up-a-nationwide.

National Weather Service Western Region Headquarters, 2020: National Oceanic and Atmospheric Administration Service Assessment: November 2018 Camp Fire. Tech. rep. URL https://www.weather.gov/media/publications/assessments/sa1162SignedReport.pdf.

NESDIS, 2021: A Model that Predicts the Spread of Wildfire Smoke Becomes Operational | NOAA National Environmental Satellite, Data, and Information Service (NESDIS). URL https://www.nesdis.noaa.gov/content/model-predicts-spread-wildfire-smoke-becomes-operational.

O'Neill, S., and S. Raffuse, 2021: Advances in satellite data for wildfire smoke forecasting. *EOS*, **102**, doi:https://doi.org/10.1029/2021EO155076.

Palinkas, L. A., 2020: The California Wildfires. *Global Climate Change, Population Displacement, and Public Health: The Next Wave of Migration*, L. A. Palinkas, Ed., Springer International Publishing, Cham, 53–67, doi:10.1007/978-3-030-41890-8_4, URL https://doi.org/10.1007/978-3-030-41890-8_4.

Powers, J. G., and Coauthors, 2017: The Weather Research and Forecasting Model: Overview, System Efforts, and Future Directions. *Bulletin of the American Meteorological Society*,

**98 (8)**, 1717–1737, doi:10.1175/BAMS-D-15-00308.1, URL https://journals.ametsoc.org/view/journals/bams/98/8/bams-d-15-00308.1.xml, publisher: American Meteorological Society Section: Bulletin of the American Meteorological Society.

Reid, C. E., M. J. Barlage, F. H. Johnston, M. Jerrett, J. R. Balmes, and C. T. Elliott, 2016: Critical Review of Health Impacts of Wildfire Smoke Exposure. *Environmental Health Perspectives*, **124 (9)**, 1334–1343, doi:10.1289/ehp.1409277, URL https://ehp.niehs.nih.gov/doi/10.1289/ehp.1409277, publisher: Environmental Health Perspectives.

Saide, P. E., J. Kim, C. H. Song, M. Choi, Y. Cheng, and G. R. Carmichael, 2014: Assimilation of next generation geostationary aerosol optical depth retrievals to improve air quality simulations. *Geophysical Research Letters*, **41 (24)**, 9188–9196, doi:10.1002/2014GL062089, URL https://agupubs.onlinelibrary.wiley.com/doi/abs/10.1002/2014GL062089.

SFGATE, A. G., 2018: San Francisco AQI jumps to 271 on Friday, worst air quality ever recorded in the city. URL https://www.sfgate.com/california-wildfires/article/how-bad-is-air-in-sf-bay-area-smoke-breathe-record-13400047.php, section: California Wildfires.

Stavroulas, I., and Coauthors, 2020: Field Evaluation of Low-Cost PM Sensors (Purple Air PA-II) Under Variable Urban Air Quality Conditions, in Greece. *Atmosphere*, **11 (9)**, 926, doi:10.3390/atmos11090926, URL https://www.mdpi.com/2073-4433/11/9/926, number: 9 Publisher: Multidisciplinary Digital Publishing Institute.

The Mercury News, 2020: Spare the Air record official after Bay Area’s latest alert extended through Saturday. URL https://www.mercurynews.com/2020/10/08/record-year-for-spare-the-air-alerts-official-after-bay-areas-latest-is-extended-through-saturday.

Wang, X., 2010: Incorporating Ensemble Covariance in the Gridpoint Statistical Interpolation Variational Minimization: A Mathematical Framework. *Monthly Weather Review*, **138 (7)**, 2990–2995, doi:10.1175/2010MWR3245.1, URL https://journals.ametsoc.org/view/journals/mwre/138/7/2010mwr3245.1.xml, publisher: American Meteorological Society Section: Monthly Weather Review.

Wettstein, Z. S., S. Hoshiko, J. Fahimi, R. J. Harrison, W. E. Cascio, and A. G. Rappold, 2018: Cardiovascular and Cerebrovascular Emergency Department Visits Associated With Wildfire Smoke Exposure in California in 2015. *Journal of the American Heart Association: Cardiovascular and Cerebrovascular Disease*, **7 (8)**, doi:10.1161/JAHA.117.007492, URL https://www.ncbi.nlm.nih.gov/pmc/articles/PMC6015400/.

Ye, X., and Coauthors, 2021: Evaluation and intercomparison of wildfire smoke forecasts from multiple modeling systems for the 2019 Williams Flats fire. *Atmospheric Chemistry and Physics Discussions*, 1–69, doi:10.5194/acp-2021-223, URL https://acp.copernicus.org/preprints/acp-2021-223/, publisher: Copernicus GmbH.

## LIST OF FIGURES

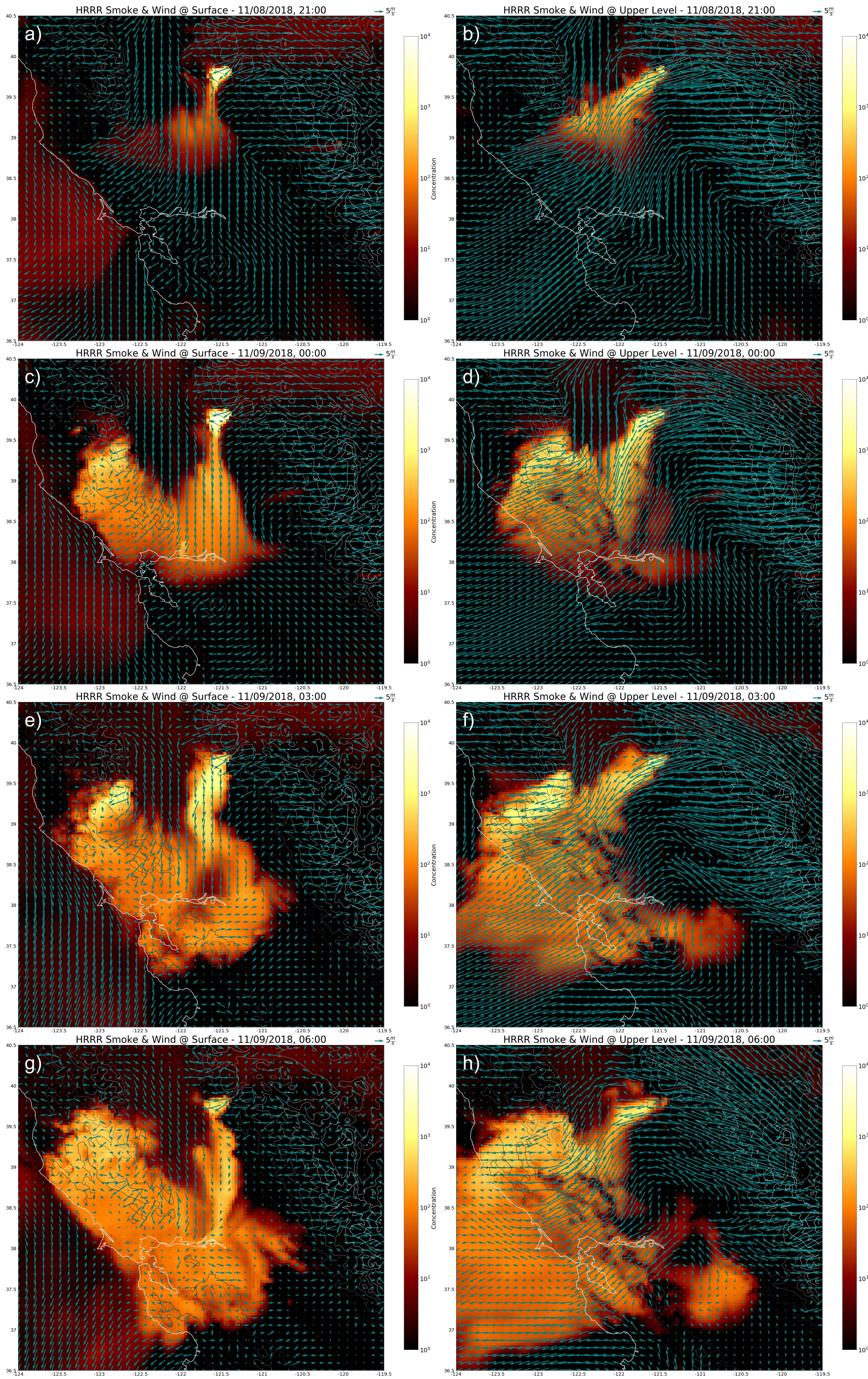


FIG. 1. Snapshot of surface smoke (left, a,c,e,g) and 1829 m AGL smoke (right, b,d,f,h) concentrations (PM2.5 $\mu$g/m$^3$ contours on log scale) and wind vectors (cyan) from HRRR-Smoke every 3 hours from 2100 UTC 8 November to 0900 UTC 9 Nov 2018.

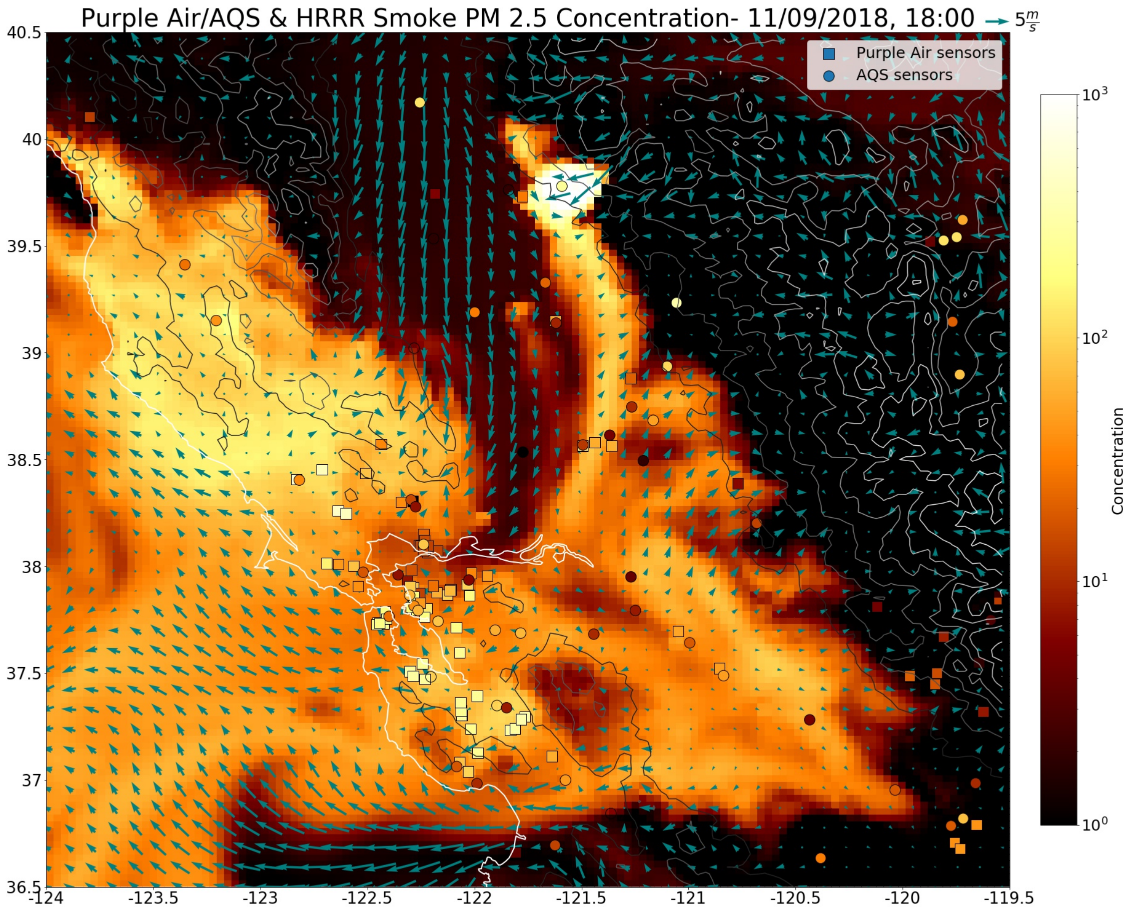


561 FIG. 2. Comparison of surface smoke concentrations (PM2.5 $\mu$g/m$^3$) from HRRR-Smoke (contours) with Purple Air (squares) and AQS (circles) stations at 1800 UTC 9 November. Surface wind vectors (cyan) also shown. Additional snapshots and a video are available in the Supplemental Material.

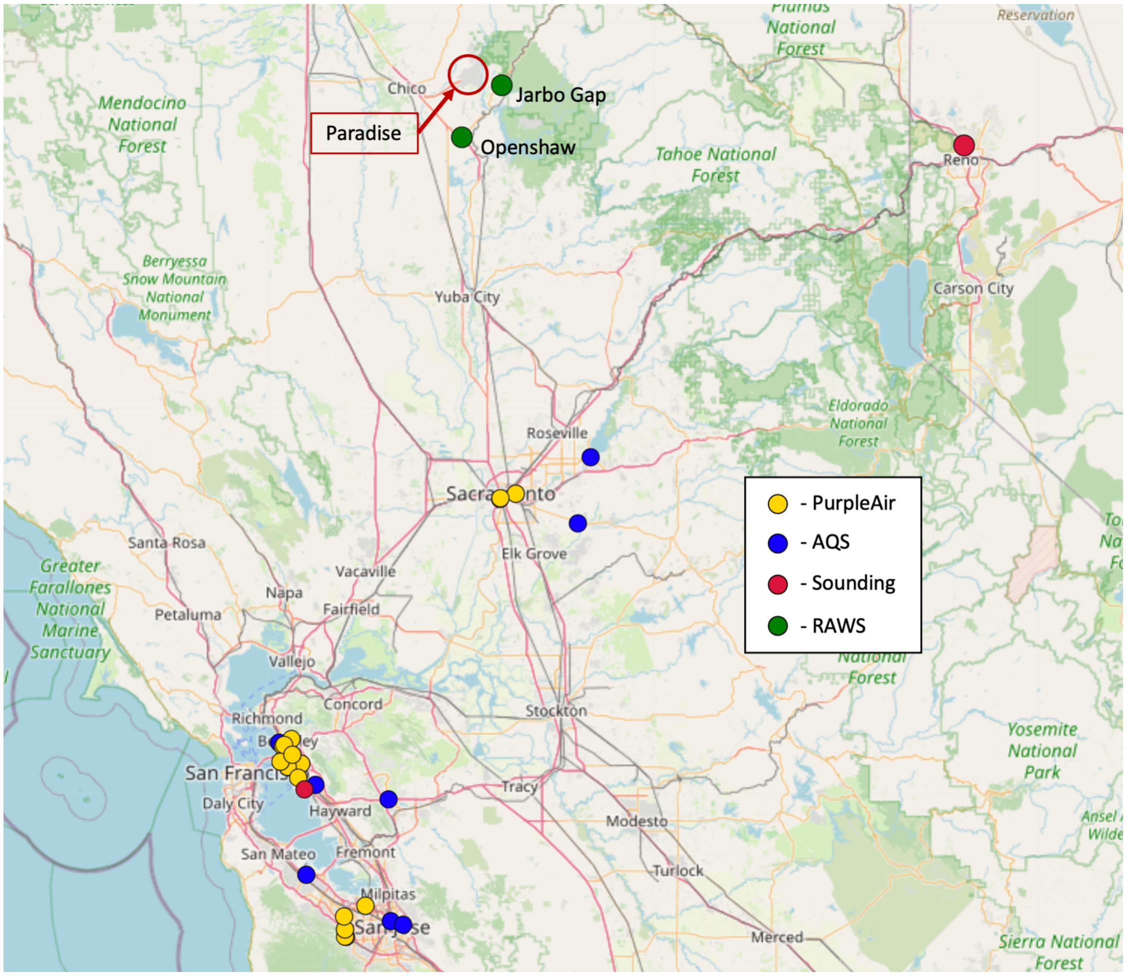


FIG. 3. RAWS, Sounding, AQS, and PurpleAir data sampling locations used in this study. The Camp Fire was located near Paradise, CA, marked by the red circle.

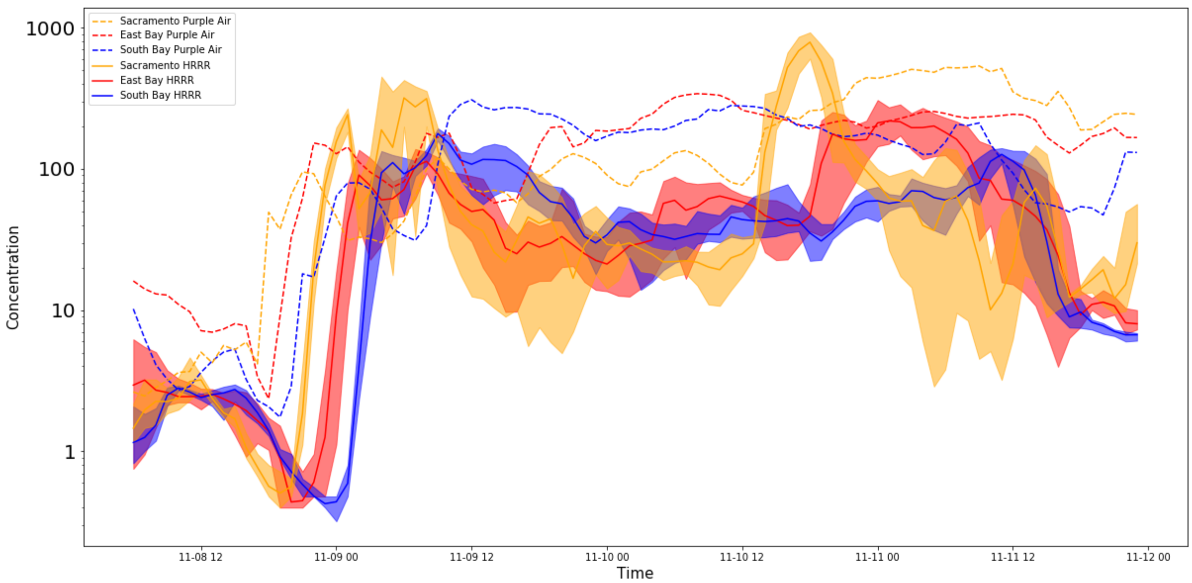


FIG. 4. Time series of PM2.5 concentrations ($\mu$g/m$^3$) from HRRR-Smoke at Sacramento, East Bay, and South Bay locations compared to averaged Purple Air sensors (dashed lines) during the initial phase of the Camp Fire event (8-12 November 2018). Solid lines are the mean over the selected area and the shaded region shows min and max) and averaged Purple Air sensors (dashed lines) during the initial phase of the Camp Fire event (8-12 November 2018).

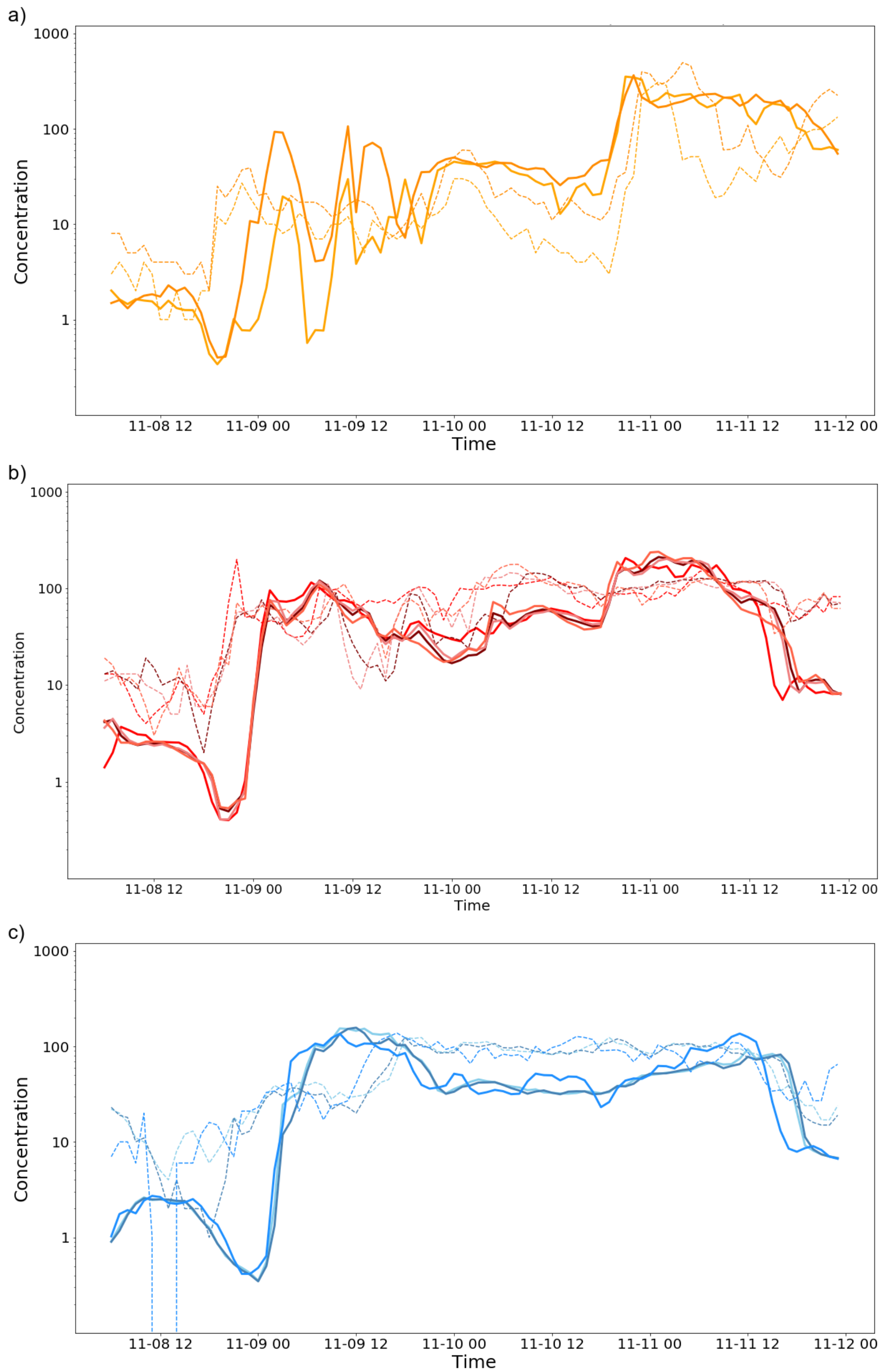


571 FIG. 5. Time series of PM2.5 concentrations ($\mu$g/m$^3$) from HRRR-Smoke and AQS stations in a) Sacramento,
572 b) East Bay, c) South Bay. Individual AQS sensors (dashed lines) and the nearest HRRR-Smoke grid point for
573 each of the sensors (solid lines) are plotted.

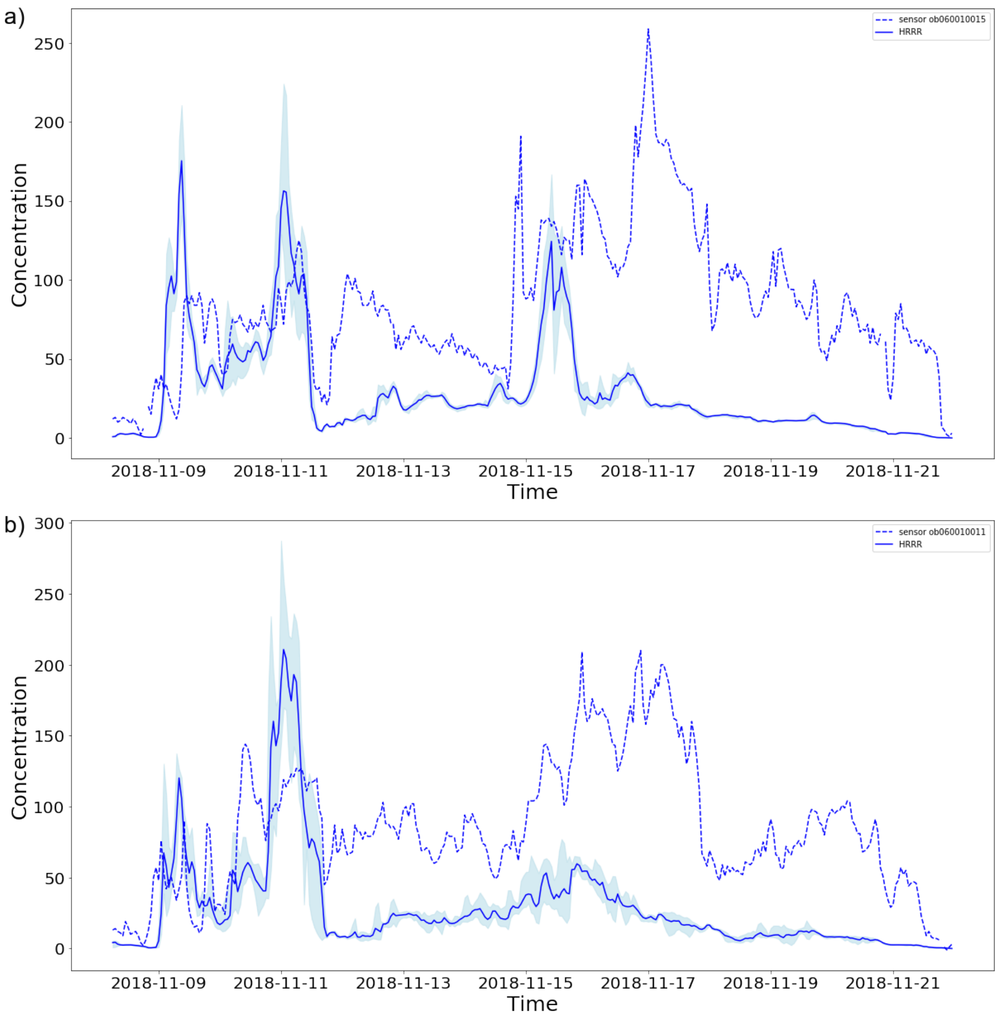


574 FIG. 6. Time series of observed PM2.5 concentrations ($\mu$g/m$^3$) at AQS stations in a) Pleasanton and b) Oakland, California compared to output from HRRR-Smoke from 8-21 November 2018. Blue shading indicates the range of values from the HRRR-Smoke model in the selected area surrounding the AQS sensor. Note the linear axis for concentration.

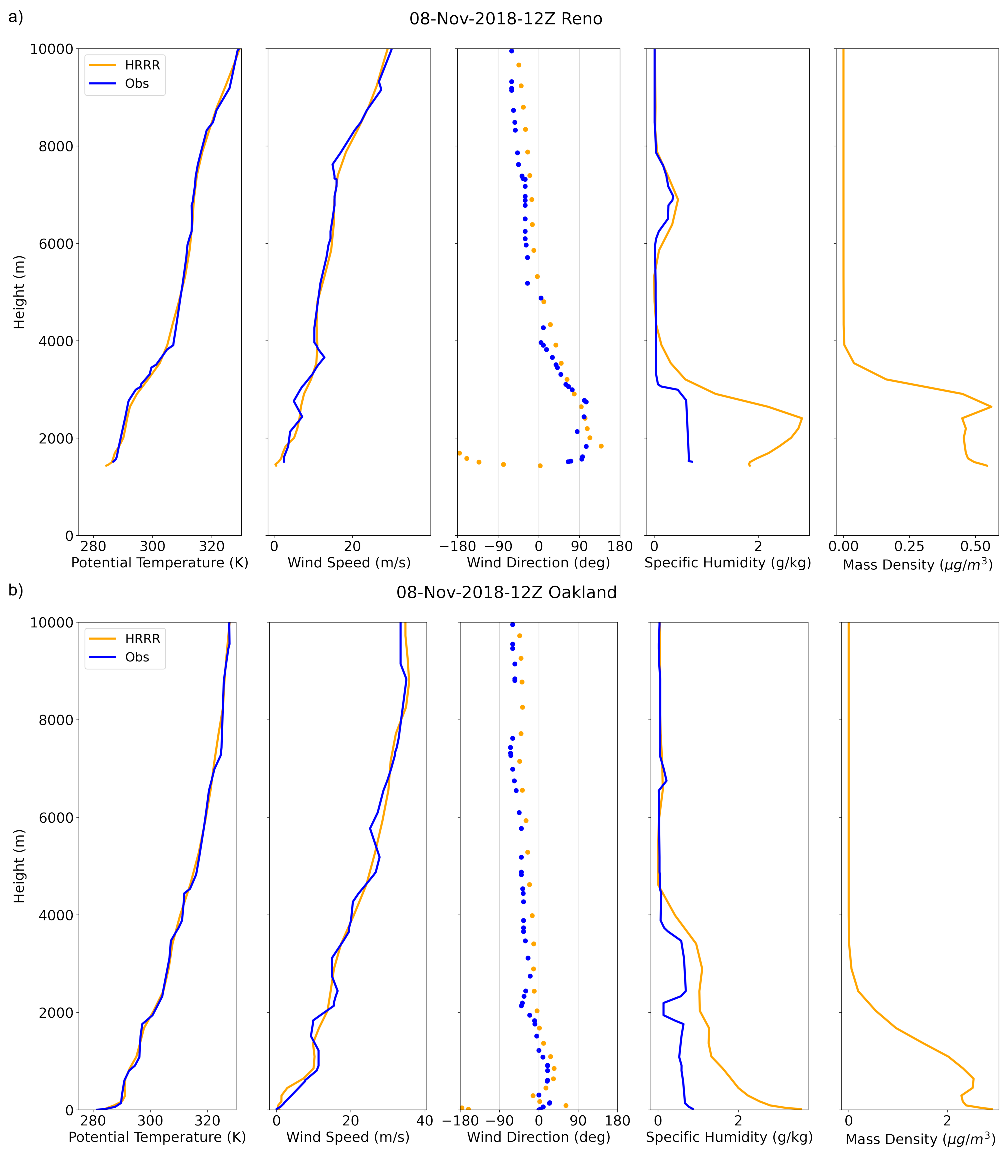


FIG. 7. Vertical profiles of potential temperature, wind speed, wind direction, specific humidity, and mass density (PM2.5 concentration) observed at a) Reno and b) Oakland at 1200 UTC 8 November 2018 compared to HRRR-Smoke model output. Note the different axis limits.

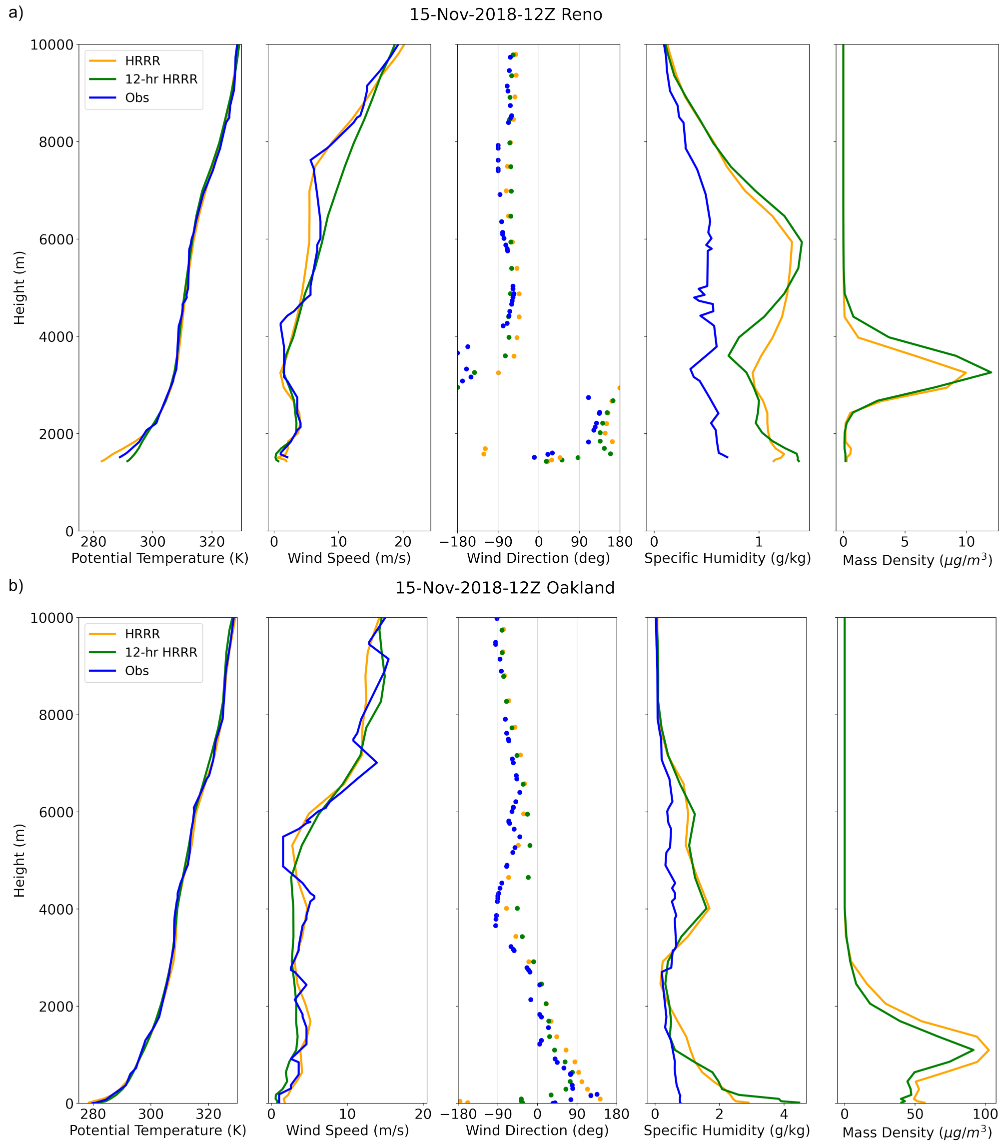


FIG. 8. As in Figure 7 but at 1200 UTC 15 November 2018. Note the different axis limits.

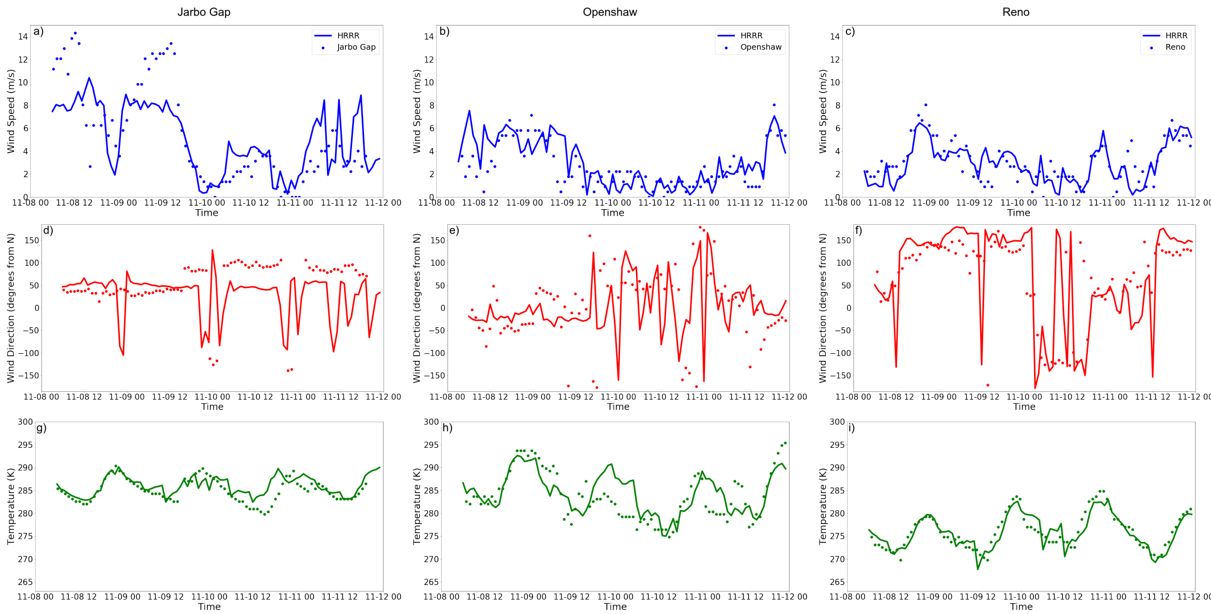


FIG. 9. Time series of wind speed (a,b,c), wind direction (d,e,f), and temperature (g,h,i) surface station data at Jarbo Gap (a,d,g), Openshaw (b,e,h), Reno (c,f,i) compared to HRRR output at nearest grid point.

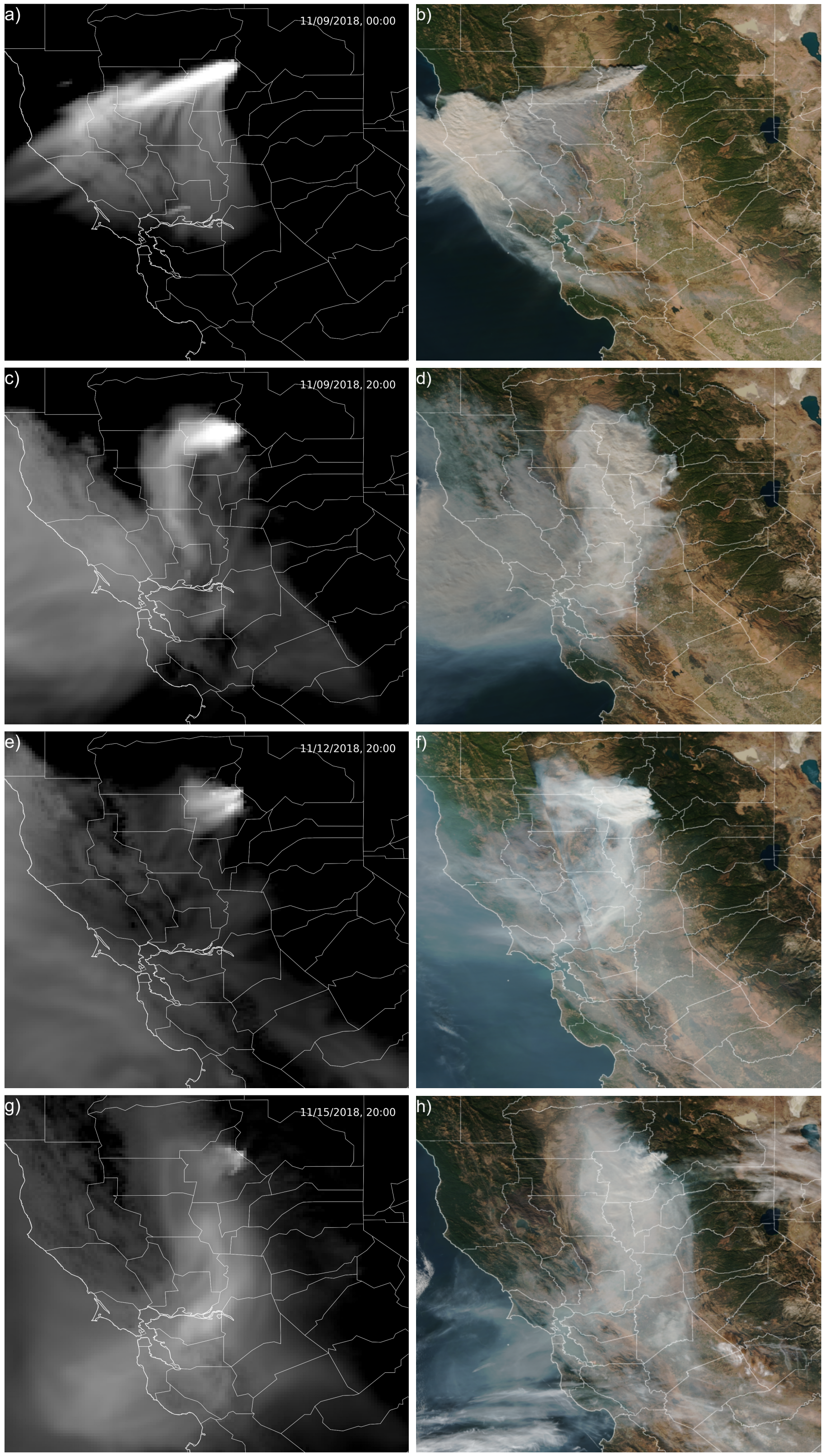


FIG. 10. HRRR-Smoke vertically integrated smoke (left) compared to Suomi NPP visible images (right). a,b) 8 November, c,d) 9 November, e,f) 12 November, g,h) 15 November 2018. HRRR-Smoke output is shown at 2000 UTC, which roughly matches the satellite crossover times, except for the first HRRR-Smoke image which is shown at 0000 UTC 9 November to account for the delay in fire ignition in the model.

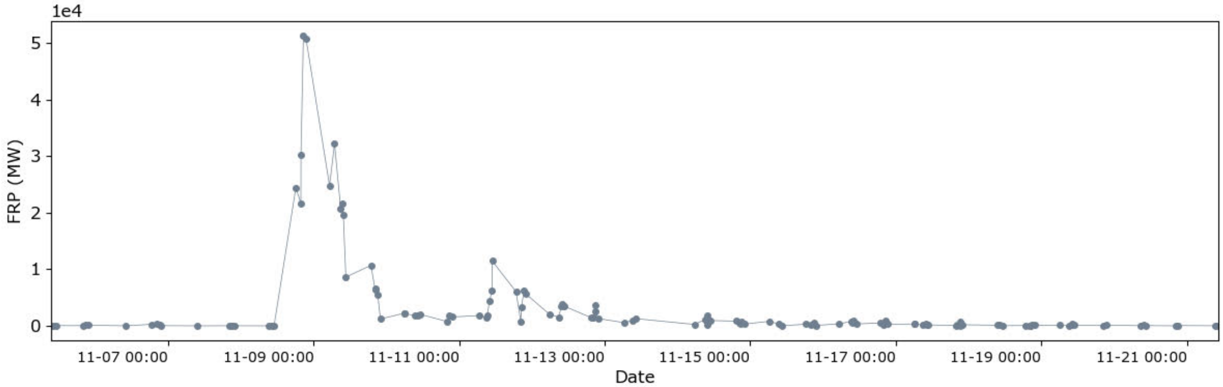


FIG. 11. Time series of the instantaneous fire radiative power for the Camp fire, detected by the two VIIRS and two MODIS instruments, spatially aggregated for the entire Camp Fire area.

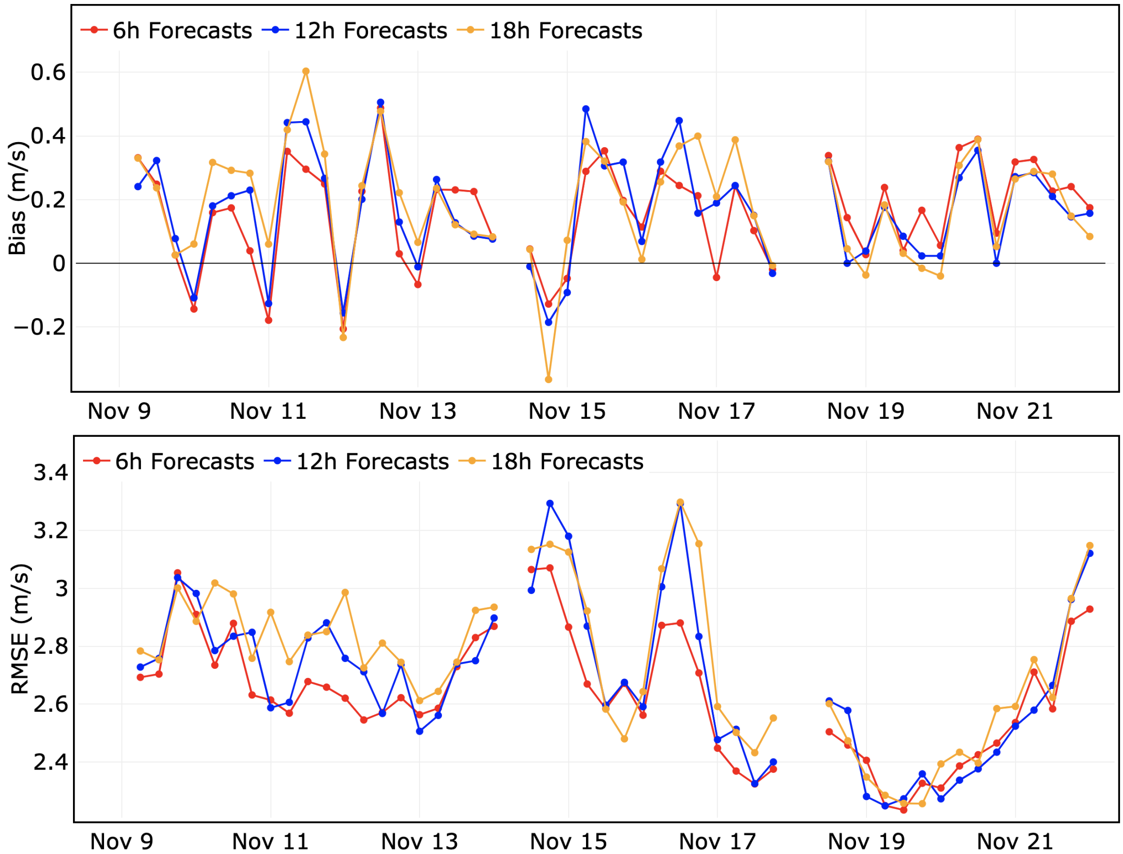


Fig. A1. Bias and RMSE plots for 10-m wind speed from 9-22 November 2018 comparing HRRR-Smoke output with all METAR surface stations in the northwest continental US.

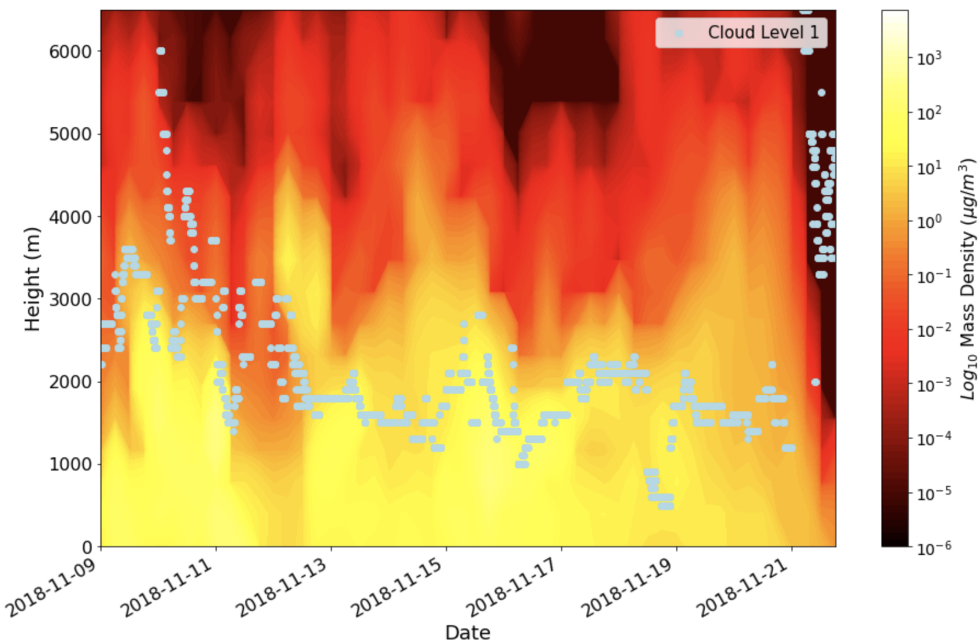


Fig. A2. Time-height contours of HRRR-Smoke PM2.5 concentration overlaid with the first cloud level from Oakland airport METAR ceilometer data (dots).

# Supplemental Material for "High-resolution smoke forecasting for the 2018 Camp Fire in California"

July 28, 2021

## 1 Evolution of HRRR-Smoke PM2.5 concentrations compared to PurpleAir and AQS sensors - video

The video is included in the .zip file and is also directly linked here.

## 2 Evolution of HRRR-Smoke PM2.5 total column smoke - video

The video is included in the .zip file and is also directly linked here.

## 3 Comparison of HRRR-Smoke PM2.5 with Purple Air and AQS sensors

## 4 Additional comparisons with radiosonde data at Oakland

## 5 Satellite images and fire radiative power - time sequence

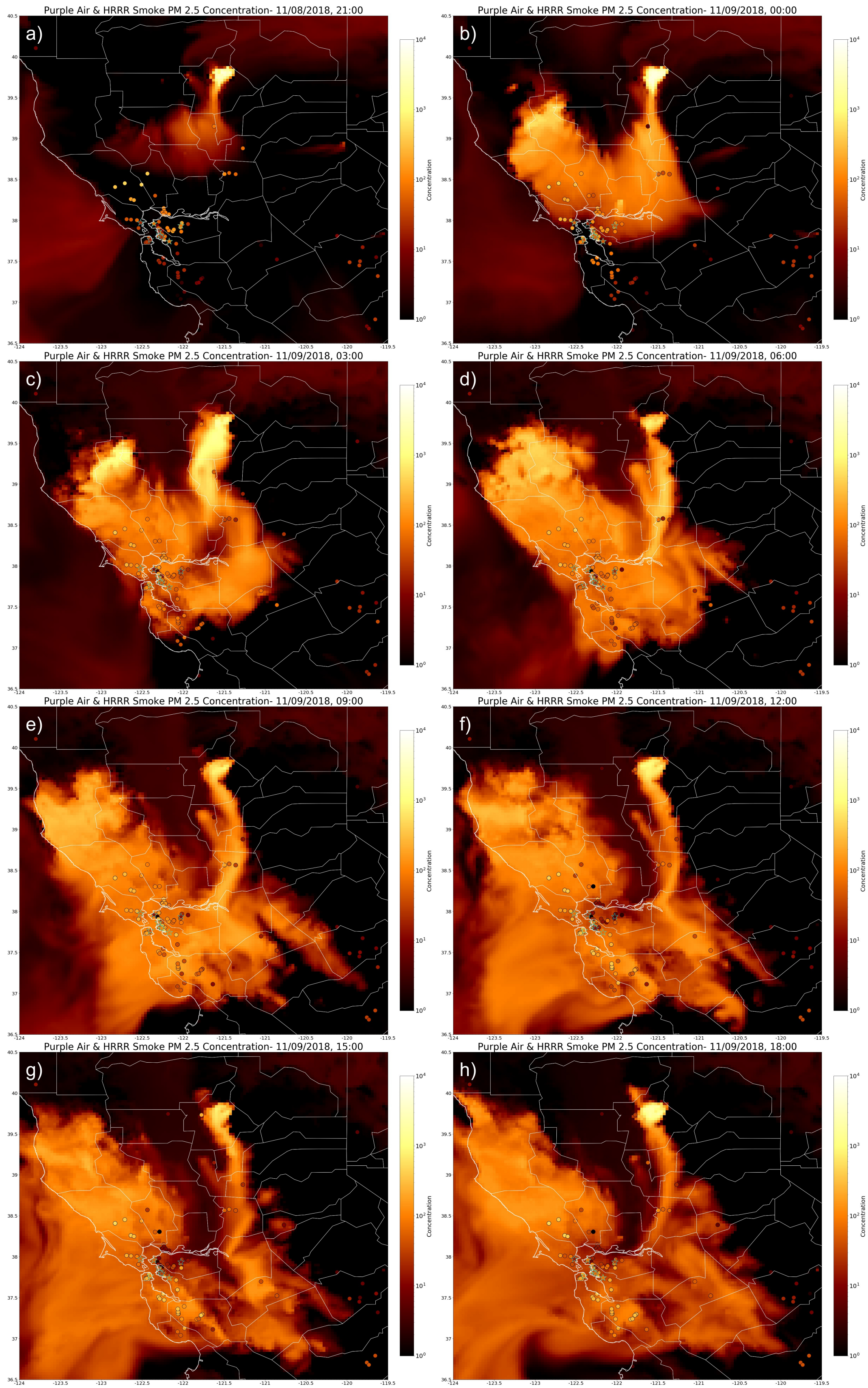


Figure 1: Comparison of surface smoke concentrations (PM2.5 $\mu g/m^3$) from HRRR-Smoke (contours) with Purple Air (squares) and AQS (circles) stations every 3 hours from 2100 UTC 8 November to 1800 UTC 9 November.

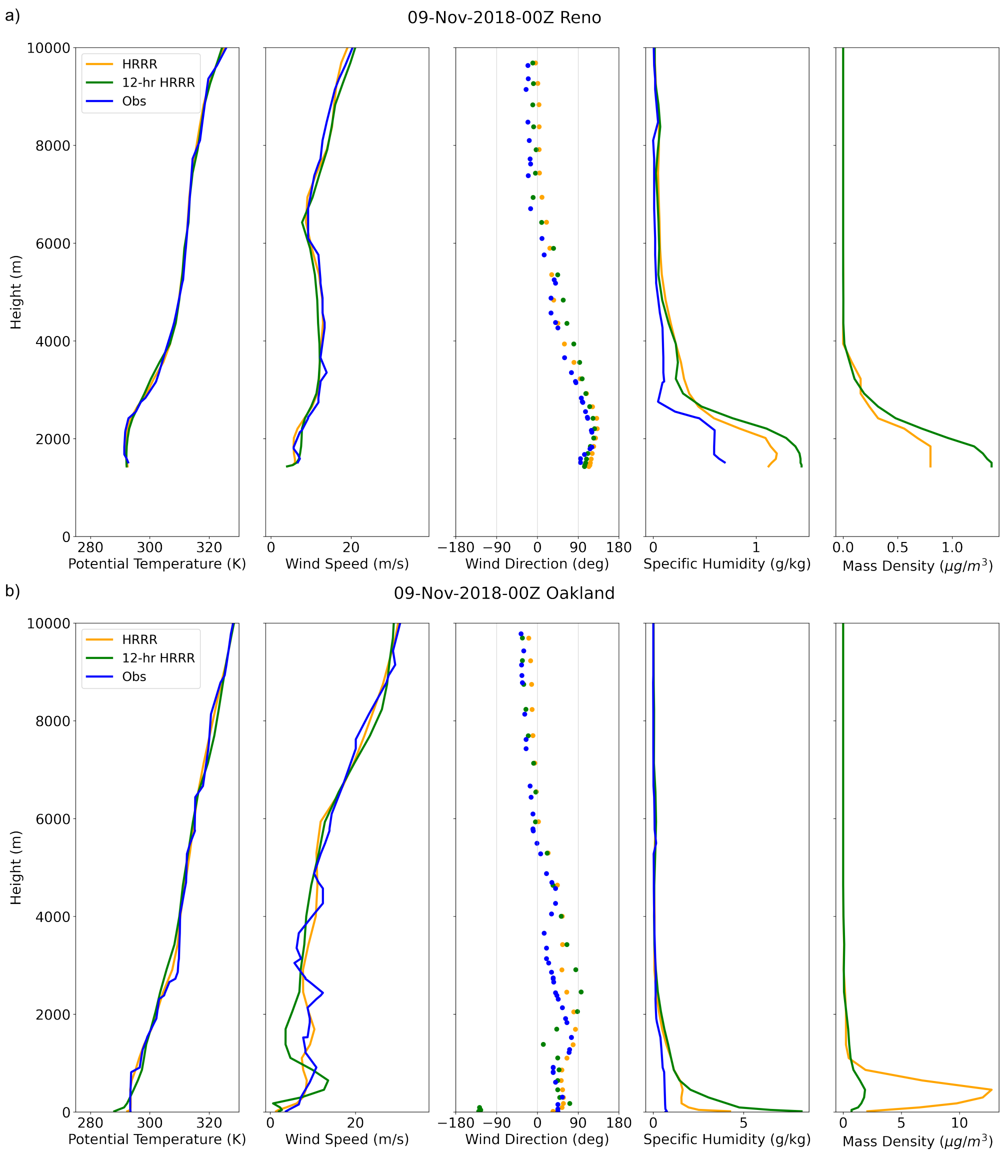


Figure 2: Vertical profiles of potential temperature, wind speed, wind direction, specific humidity, and mass density (PM2.5 concentration) observed in a) Reno and b) Oakland at 0000 UTC 9 November 2018 compared to HRRR-Smoke model output. Note the different axis limits.

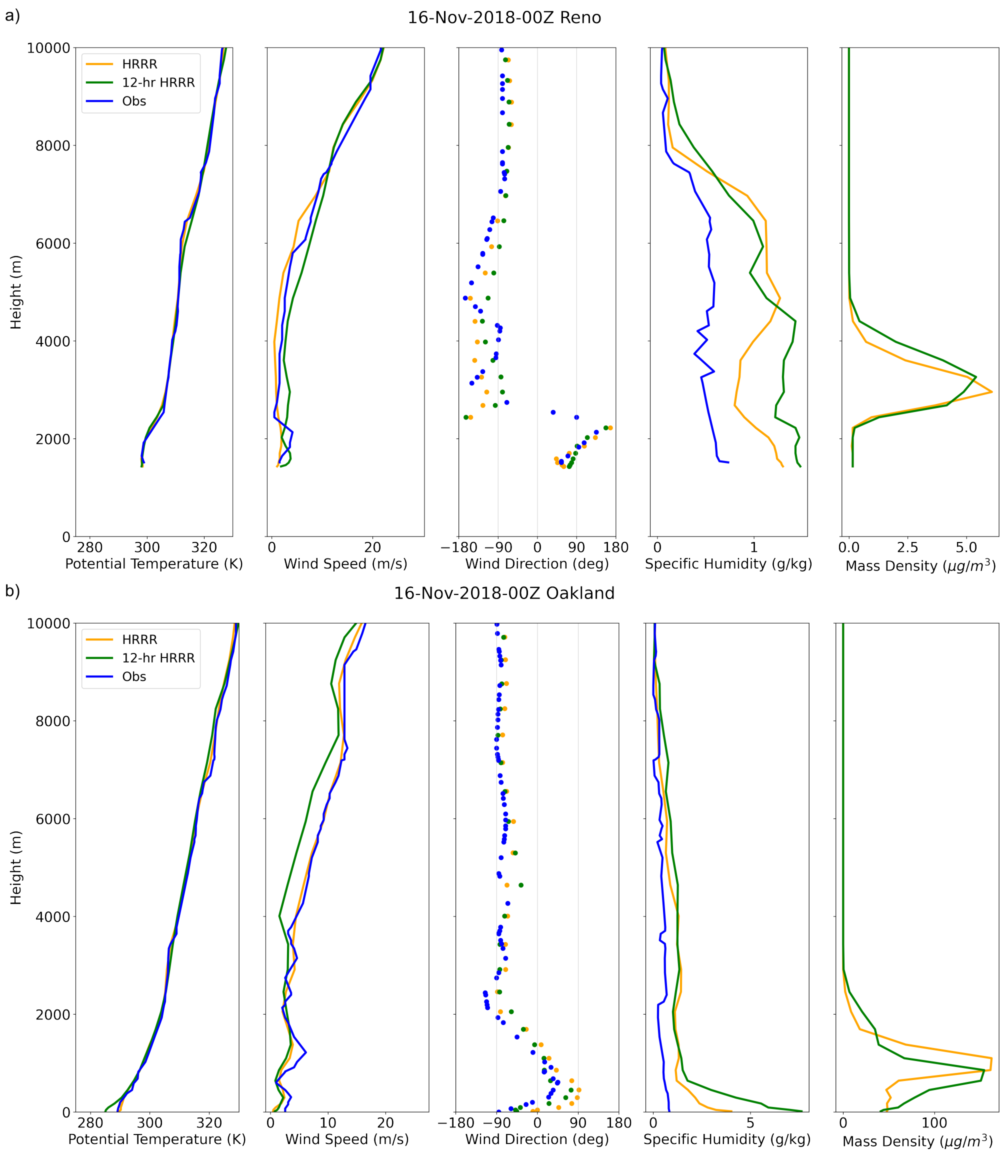


Figure 3: As in Figure S2 but at 0000 UTC 16 November 2018. Note the different axis limits.

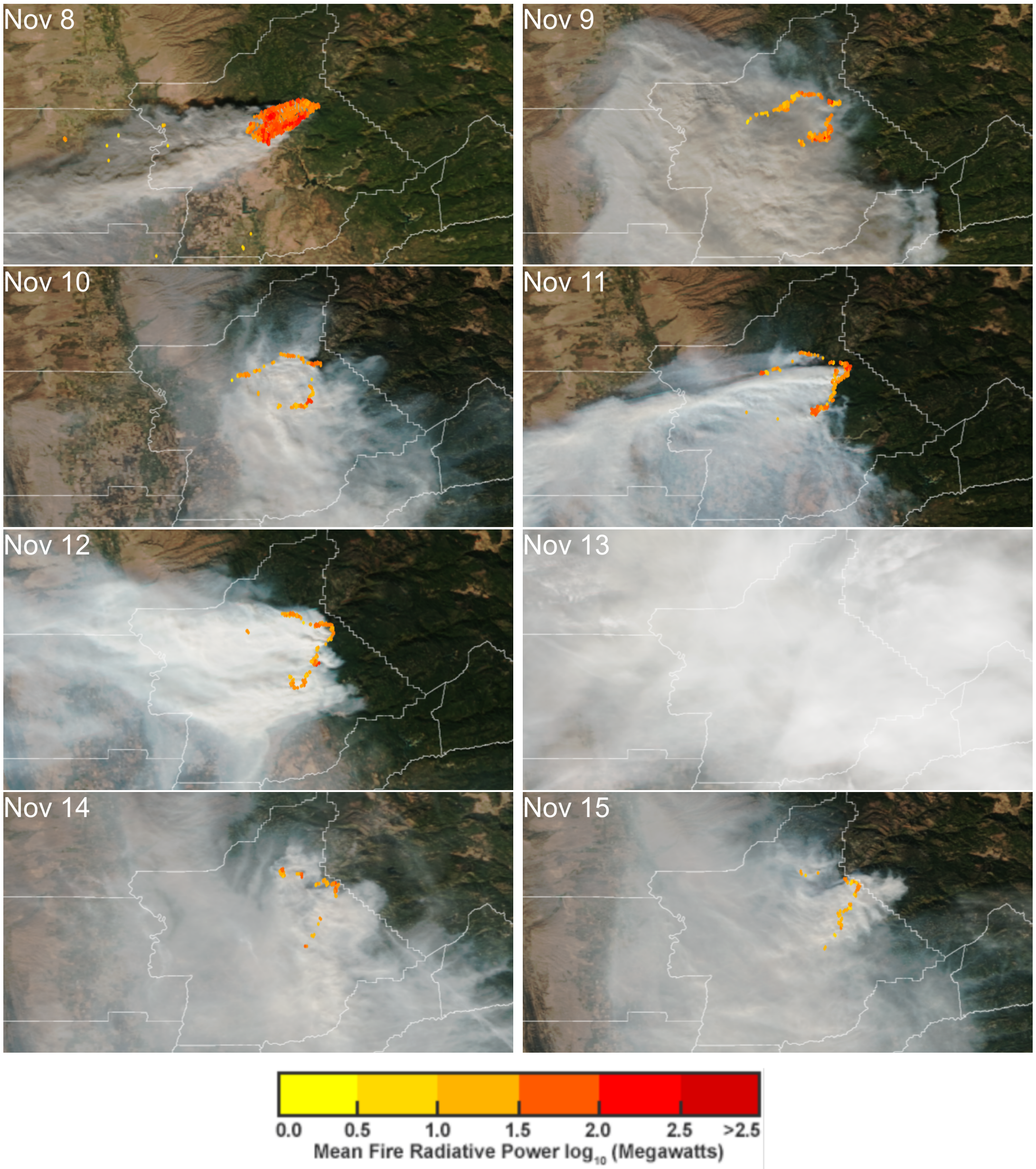


Figure 4: Daytime composite Suomi NPP VIIRS I-band Fire Radiative Power data over a VIIRS true color image around the Camp Fire complex in November 2018. Images from JSTAR Mapper `https://www.star.nesdis.noaa.gov/jpss/mapper/`, where NOAA-20 data as well as nighttime data are also available.

Supplemental Material zip file

Click here to access/download
**Supplemental Material**
supplemental.zip